

OPEN

Continental degassing of helium in an active tectonic setting (northern Italy): the role of seismicity

Dario Buttitta^{1*}, Antonio Caracausi^{1*}, Lauro Chiaraluce², Rocco Favara¹, Maurizio Gasparo Morticelli³ & Attilio Sulli³

In order to investigate the variability of helium degassing in continental regions, its release from rocks and emission into the atmosphere, here we studied the degassing of volatiles in a seismically active region of northern Italy ($M_{w\text{MAX}} = 6$) at the Nirano-Regnano mud volcanic system. The emitted gases in the study area are CH_4 -dominated and it is the carrier for helium (He) transfer through the crust. Carbon and He isotopes unequivocally indicate that crustal-derived fluids dominate these systems. An high-resolution 3-dimensional reconstruction of the gas reservoirs feeding the observed gas emissions at the surface permits to estimate the amount of He stored in the natural reservoirs. Our study demonstrated that the *in-situ* production of ^4He in the crust and a long-lasting diffusion through the crust are not the main processes that rule the He degassing in the region. Furthermore, we demonstrated that microfracturation due to the field of stress that generates the local seismicity increases the release of He from the rocks and can sustain the excess of He in the natural reservoirs respect to the steady-state diffusive degassing. These results prove that (1) the transport of volatiles through the crust can be episodic as function of rock deformation and seismicity and (2) He can be used to highlight changes in the stress field and related earthquakes.

Large-scale vertical transport of fluids through the continental crust is not always dominated by steady-state diffusion processes but it can be also advective and episodic^{1–4}. It has been recognized that in continental regions volatiles degassing mainly occurs in areas characterised by extensional tectonic and often coincides with seismically active zones⁵. This correspondence has been related to the enhanced permeability of the extensional tectonic discontinuities⁶. However, it has been also observed that variations of the volatiles degassing rate are earthquake-related, and are frequently post-seismic^{7–9}. Thus, fluids geochemistry provides evidences of the episodic large-scale transport of volatiles. Even if the flux of the major natural gases (i.e., CO_2) towards the atmosphere is measured at surface it is difficult to constrain the processes controlling its variability because fluids are often reactive (e.g. water-gas-rock interaction) and several processes work concomitantly during the fluids transfer through the crust¹⁰. Therefore, in order to figure out the relationships between fluids and earthquakes generation processes, at the base of a possible modern earthquake forecast approach, it is fundamental to unravel the processes causing and regulating the fluids flux and chemistry.

Because of their chemical properties, noble gases contribute to retrace the degassing history of the Earth and the evolution of the atmosphere^{11–15}. Furthermore, for investigating the mechanism controlling the transport of fluids in continental region, He, the lightest noble gas, is largely used because its sources (air, crust and mantle) are well resolvable by the use of the isotopic ratio ($^3\text{He}/^4\text{He}$)¹⁴. In fact, He is characterized by two isotopes: ^3He , which is a primordial component and it is mainly stored in the mantle, and ^4He that is continuously produced by the U and Th decay, so its amount stored into minerals and rocks progressively increases over geological time. Melting and volatiles release from magma are the main processes that control He outgassing from the mantle. Instead, degassing of He produced in the crust occurs under different conditions mainly consisting of two stages acting at different scales: (a) the release of the volatiles from the mineral/rocks; (b) their transport towards the surface¹³. It is recognized that the crustal fluids are dominated by ^4He , on the contrary, mantle-derived fluids show an excess of ^3He (MORB mantle $^3\text{He}/^4\text{He}$ is $8 \pm 1 \text{ Ra}$, where Ra is the isotopic ratio in atmosphere, $1.382 \pm 0.005 \times 10^{-6}$)^{16,17} respect to the crustal-derived fluids. He is also found in considerable quantities in some natural-gas reservoirs,

¹Istituto Nazionale di Geofisica e Vulcanologia, sezione di Palermo, Palermo, Italy. ²Istituto Nazionale di Geofisica e Vulcanologia, Osservatorio Nazionale Terremoti, Roma, Italy. ³Dipartimento di Scienze della Terra e del Mare, Università di Palermo, Palermo, Italy. *email: buttittadario@gmail.com; antonio.caracausi@ingv.it



Figure 1. Study area. (a) Geographical framework with sampled sites⁷³. (b) Some photos of Nirano and Regnano mud volcanoes during the 2018 sample campaign.

where it can remain stored for millions of years^{18,19}. The continental ^4He degassing shows spatial and temporal variability at regional scale¹, so it is an efficient tool for evaluating the role of tectonics in enhancing the crustal scale mass transport and decipherer the mechanisms of the transfer of volatiles^{1,20–23}. Changes of physical properties of rocks can modify the release and transfer of volatiles through the crust²⁴. For instance, rock deformation produces new (micro) fractures enhancing the release of the trapped volatiles (e.g., He) and as a consequence the fraction of volatiles released from the rocks during deformation, increases with the rock volume changes (dilatancy processes). However, even if some experimental studies show the existence of a direct link between rock deformation/fracturation and the release of He^{25,26}, there are only a few of applications in natural systems^{21,27,28}. In this study, we investigated the origin and processes controlling the transfer of He through the crust in a seismically active region of the Northern Apennines (Fig. 1), to establish the possible contribution of the tectonic activity in enhancing the release of volatiles accumulated in the rock over time and more specifically, how earthquakes occurrence may contribute to the episodic volatiles degassing. To this end we collect fluids from mud volcanoes (Fig. 1a,b) and we analyse their chemical and isotopic composition (He , $\delta^{13}\text{C}-\text{CO}_2$, $\delta^{13}\text{C}-\text{CH}_4$, $\delta^2\text{H}-\text{CH}_4$) to figure out the origin of the outgassing volatiles and the process controlling the crustal degassing. Once verified that the volatiles comes from deep natural reservoirs, we reconstructed the reservoirs volume to estimate the total amount of He stored in these natural traps. The balance between input and output of He in the reservoirs allow us to unravel the processes that control the crustal degassing from He production until its transfer towards the surface, giving also insights to the role and modality of tectonic and seismicity in the vertical transferring of fluids (diffusive vs. advective and episodic).

Results

In the northern Apennines (Italy) the mud volcanoes are distributed along the external sector of the fold-and-thrust belt (Fig. 1).

This region is considered a reference area to study fluid venting processes in an active fold-and-thrust belt²⁹ and the fluids geochemistry is used as a potential indicator of impending local earthquakes³⁰. The seismicity is concentrated in the crust and at local scale the maximum magnitude is 6.0 (<https://emidius.mi.ingv.it>). Furthermore, it is recognized that the fluid output from the mud volcanoes increased just after the earthquakes^{9,31–33}.

Previous investigations highlighted that the gases emitted from the mud volcanoes are CH_4 -rich³⁴ and they are fed by two reservoirs that are strongly different in dimension and vertically separated³⁵. At the regional scale, the studied mud volcanoes are localised at the top of the anticlines (Fig. 1a), particularly in joints perpendicular

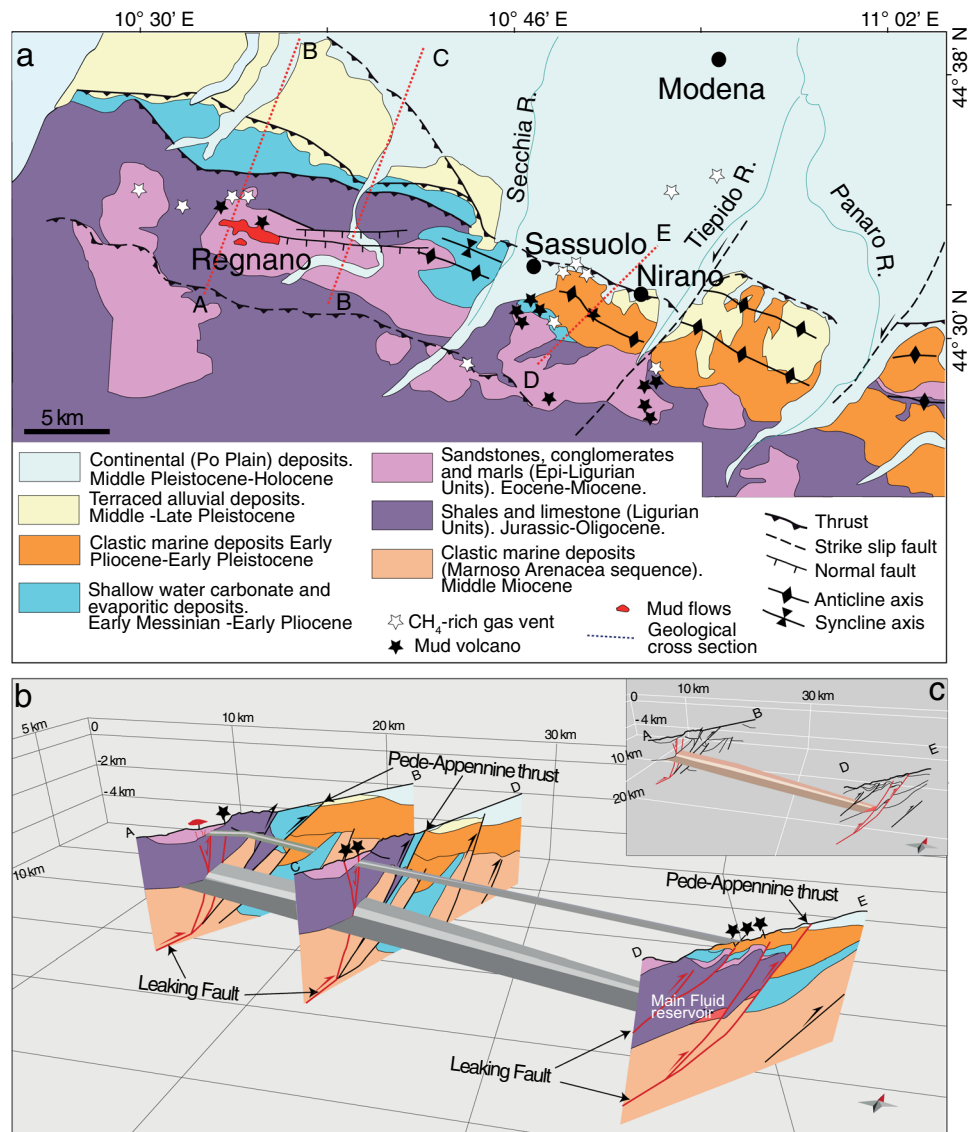


Figure 2. A general overview of the area with the geological units of the zone of interest (a) a view of the shallow and deep reservoirs by reconstruction carried out with Move 2015.1 software (b) deep reservoir and the system of faults that crosses it (c).

to the axis of the fold, where the impermeable cover allows pore fluid pressure build-up (close to lithostatic magnitudes)³⁵. Mud volcanoes are placed along active normal faults (Fig. 2a), allowing a vertical migration of CH₄ coming from deep sources (>3–6 km)³⁶.

In this region mud volcanism can be potentially triggered by fault failure cycles and the overpressured fluids released during faulting³⁵. Furthermore, the relatively quiescent but continuous activity of these mud volcanoes could instead reflect a short-lived leakage of overpressured fluids along permeable fractures/faults. We are therefore in the presence of a study-case site to investigate the mechanisms of fluid transfer through the crust and the possible relationships between degassing of crustal fluids and rocks deformation and seismicity.

Fluids geochemistry. We collected gas samples from four different mud volcanoes areas (Fig. 1): Nirano, Montegibbio, Regnano and Casola. Nirano - Montegibbio sites are located 3.5 km apart, while Regnano - Casola only 2.0 km. Hereafter, we named Nirano-Montegibbio sites as the Nirano system and Regnano-Casola sites as the Regnano system. We analysed the fluids for defining the gas chemistry (He, H₂, O₂, N₂, CO, CH₄, CO₂ and C₂H₆) and the isotopic composition of He (³He/⁴He), ²⁰Ne, C of both CH₄ and CO₂ and H of CH₄ (Table 1).

According to previous investigations^{36–38} the outgassing fluids from the Nirano and Regnano systems are CH₄ dominated (96.7–98.3%). CO₂ is up to 1.04%, O₂ and N₂ up to 0.09% and 1.27% respectively; He is in traces (up to 23 ppm vol.). The low concentrations of O₂ and N₂ indicate that the collected gases suffer low air contaminations (Fig. 3a).

Site	Sampling Date	Lat	Long	O ₂ (%)	N ₂ (%)	CH ₄ (%)	CO ₂ (%)	C ₂ H ₆ (ppm)	He (ppm)	²⁰ Ne (ppm)	⁴ He/ ²⁰ Ne	(R/Ra) _c	Err+/-	δ ¹³ C-CO ₂	δ ¹³ C-CH ₄	δ ¹³ D-CH ₄	C(tot)/ ⁴ He
Nirano	29/09/2018	N 44° 30' 49.57"	E 10° 49' 32.13"	0.01	0.34	98.26	0.54	381	18	0.029	636.47	0.01	1.27 × 10 ⁻⁴	+18.61	-47.2	-173	5.4 × 10 ⁻⁴
Nirano 2	29/09/2018	N 44° 30' 46.14"	E 10° 49' 16.90"	0.05	0.55	98.18	0.53	374	18	0.098	187.02	0.01	1.06 × 10 ⁻⁴	+13.77	-46.2	-179	5.4 × 10 ⁻⁴
Regnano	29/09/2018	N 44° 33' 28.75"	E 10° 34' 33.30"	0.09	0.62	97.74	1.04	1800	24	0.394	59.37	0.01	7.78 × 10 ⁻⁵	+18.41	-46.7	-170	4.2 × 10 ⁻⁴
Casola	29/09/2018	N 44° 34' 26.56"	E 10° 33' 57.94"	0.02	0.56	96.74	0.97	587	20	0.070	354.35	0.01	1.00 × 10 ⁻⁴	+16.08	-45.1	-176	4.8 × 10 ⁻⁴
Montegibbio	29/09/2018	N 44° 30' 58.13"	E 10° 46' 37.14"	bdl	01.27	97.08	0.27	135	37	0.171	215.32	0.01	9.67 × 10 ⁻⁵	n.d.	-46.2	-178	7.9 × 10 ⁻⁴

Table 1. Chemical and isotopic composition of the venting gases from the mud volcanoes of Nirano and Regnano areas.

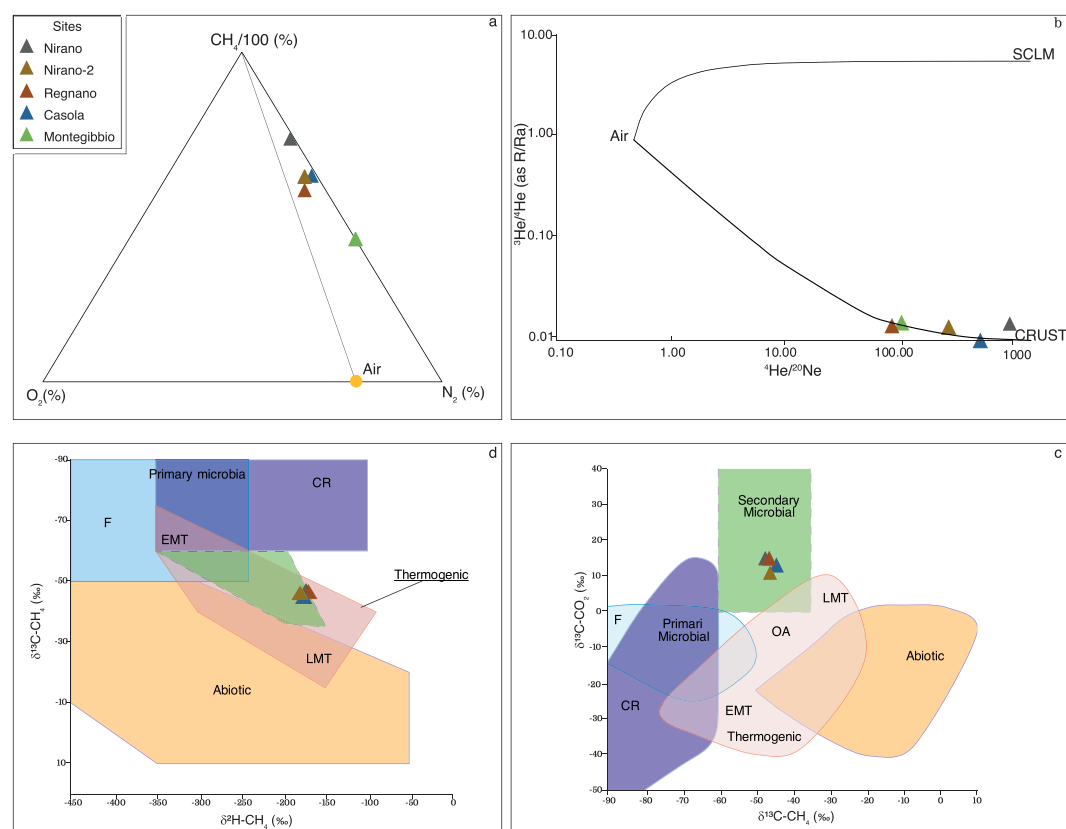


Figure 3. O₂-N₂-CH₄/100 ternary diagram for the gas samples investigated. All the gases are CH₄-dominated and are not along the mixing line between a pure CH₄ end-member and air showing that the sampled gases are not air-contaminated. **(a)** A correlation diagram between the ³He/⁴He and ⁴He/²⁰Ne ratios for the gas samples investigated. The whole black lines show the mixing lines between mantle-derived helium and between radiogenic helium with the Air. The mantle end-member is the Sub Continental Lithospheric Mantle (SCLM, 6.1 ± 0.9 Ra)⁷⁴. **(b)** Genetic diagrams of δ¹³C-CH₄ versus δ¹³C-CO₂ **(c)** and methane genetic diagrams based on δ²H-CH₄ versus δ¹³C-CH₄. **(d)** T – thermogenic, A – abiogenic, CR – CO₂ reduction, F – fermentation, OA – oil-associated thermogenic gas, LMT – late mature thermogenic gas, EMT – early mature thermogenic gas, SM – Secondary Microbial. The gaseous hydrocarbons are a mixture of secondary biogenic methane and primary and secondary thermogenic gases. The associated oils show both early and late maturities. These evidences account for different generation and migration steps, depending on burial conditions and deformation time³⁹.

The He isotopic ratios are 0.01–0.03 Ra, that is the typical range of the crustal radiogenic He (Fig. 3b). The ⁴He/²⁰Ne ratios in the collected fluids are from 59.4 to 636.5 and these values are more than 2 order of magnitude higher than the same ratio in air (⁴He/²⁰Ne_{AIR} = 0.318)¹⁴ supporting the low atmospheric component in the gases from the Nirano and Regnano systems (Fig. 3a,b). Hence, the outgassing He from the mud volcanoes systems is dominated by radiogenic ⁴He that is produced by U and Th decay in the crust¹⁴. The C and H isotopic composition of CH₄ is in a good agreement with previous results highlighting the thermogenic nature of CH₄ (Fig. 3c and

	Calculation of the initial gas in place		
	Main		Secondary
Reservoir Conditions	Trc = 327.15 °K		Trc* = 295.75 °K
	$P_{rc}^{Litho} = 48.98 \text{ MPa}$		$P_{RC}^{Litho*} = 4 \text{ MPa}$
G.B.V. in m ³	9.49×10^9		2.69×10^8
ϕ	0.15		0.50*
(1-Sw-So)	0.75/0.85		0.10*
1/Bg in SCM/RCM	371.19		42.25
Z	1.1646		0.9244
	So = 0.10	So = 0	So = 0
Q (SCM)	3.99×10^{11}	4.5×10^{11}	5.68×10^8
Q (mol)	1.66×10^{13}	1.87×10^{13}	2.35×10^{10}
Q ⁴ He (SCM)	8.78×10^6	9.94×10^6	1.19×10^4
Q ⁴ He (mol)	3.64×10^8	4.12×10^8	4.93×10^5

Table 2. Summary of reservoirs condition and initial gas in place into the traps calculated by volumetric method. *Data from Oppo⁷⁵.

Table 1)^{37–39}. Here we report the first data of C and H isotopes of CH₄ in gases from Casola and Montegibbio sites, indicating a unique origin of CH₄ emitted from these mud volcanoes systems (Fig. 3c and Table 1). The carbon isotopic composition of CO₂ in all the studied fluids is from +13.8‰ to +18.6‰ and according to Milkov and Etiope (2018)⁴⁰ these values coupled to the isotopic composition of CH₄ indicate that CO₂ is of thermogenic origin (Table 1 and Fig. 3c,d). These results are in a good agreement with those from previous investigations³⁶ that highlighted (1) the thermogenic nature of pristine methane in the deep reservoirs, (2) an origin of CH₄ in crustal layers deeper than the reservoirs (>3–6 km) and (3) a vertical migration of CH₄ towards the surface. Considering the main component in the collected gases is CH₄ (~98%) and the average CH₄/⁴He ratio in the emitted gases is ~46000 we computed the amount of ⁴He in the two reservoirs by using the total amount of gases into the reservoirs, between 4.00×10^{11} and 4.50×10^{11} standard cubic meter (SCM) for the main reservoir, and 5.68×10^8 SCM for the shallow reservoir (Supplementary Information: gas reserves). So, the amount of ⁴He into the shallower reservoir and deep reservoirs are 4.90×10^5 moles and 3.60×10^8 – 4.20×10^8 moles respectively. The amount of ⁴He in the shallow reservoir is three order of magnitude lower than the amount in the deep reservoir (lower than 1% of ⁴He amount in the deep reservoir), so it can be considered negligible (Table 2).

He degassing. There have been many consistent estimates of the flux of ⁴He from the continental crust based on calculations of *in situ* production and steady-state release to the atmosphere by using the U and Th content in rocks, crustal thickness and total release of ⁴He. These calculations yield a crustal degassing flux of ⁴He of the order $3.3 \pm 0.5 \times 10^{10}$ (atoms \times m⁻² \times s⁻¹)^{1,15,41}. However, experimental works highlighted that the release of volatiles increases in volume of rock in an active stress field, which supports that the ⁴He degassing through the crust can be episodic in active tectonic areas^{26,42,43}. Mechanical deformation and rocks failure can break (or crack) mineral grains, causing pervasive micro-fracturing and dilation. Consequently, the rocks can increase porosities from 20% to as high as 400% prior to failure⁴⁴, open new micro-fracture surfaces, and eventually cause macroscopic failure and fracture of rocks⁴⁵. These processes lead to a release of volatiles (e.g. He) previously trapped within mineral grains along fracture networks^{46,47} and the pore fluids transport these volatiles through the crust. Here we firstly investigate if a steady state degassing is the main process that controlled the ⁴He flux to the reservoirs below the Regnano and Nirano systems over time.

He degassing: Steady-state conditions. The local stratigraphy and tectonic evolution indicates that the age of formation of the anticline hosting the main gas reservoirs below the Regnano and Nirano systems goes from 1.8 to 4.5 Ma. Over a million-year the flux of ⁴He through the Earth's crust to the atmosphere is comparable to the net *in situ* production (in steady state condition), in 30–40 km of crustal thickness⁴⁸. In order to assess if the ⁴He production in the crust and the successive migration to the natural reservoirs feeding the Nirano and Regnano systems can justify the amount of He that is stored in the reservoirs, we used a mass balance approach⁴⁹:

$${}^4\text{He} = {}^4\text{He}_{\text{Initial}} + {}^4\text{He}_{\text{Insitu}} + {}^4\text{He}_{\text{External flux}} - {}^4\text{He}_{\text{Leak-d}} - {}^4\text{He}_{\text{leak-mv}} \quad (1)$$

where ⁴He represents the amount of radiogenic helium (moles) in the reservoir at time t. It includes three input and two outputs terms. Among the input terms, ⁴He_{Initial} is the amount of ⁴He that is in the reservoir at time t-zero, ⁴He_{Insitu} the amount of radiogenic ⁴He produced in the reservoir-rocks volume since its formation (from 1.8 to 4.5 Ma), ⁴He_{External flux} is the flux from the crust below the reservoirs. ⁴He_{Leak-d} and ⁴He_{Leak-mv} are the two terms of outputs: ⁴He_{Leak-d} is the He lost by diffusion from the main reservoir over time and it is from 4.37×10^5 mol to 1.09×10^6 for a t of 1.8 Ma and 4.5 Ma respectively (Methods; gas reserves). It is up to 0.36% of the total volume of He. The second one, ⁴He_{Leak-mv}, is the He leak due to advection, and we assume that is the He emitted from the mud volcanoes. We extrapolated the current He outgassing from mud volcanoes, to the past 10⁴ years, in this time we have considered the continuous degassing (about 95 mol/y), and the possible paroxysmal activity as follows: “normal” eruption (10 times the continuous, every year) and “strong” eruption (100 times the continuous, once

	Thickness (km)	Density (g/cm ³)	RRM-Regional*		RRM-Global*	
			U (ppm)	Th (ppm)	U (ppm)	Th (ppm)
Sediments	10	2.21	0.78 ± 0.20	1.98 ± 0.44	1.68 ± 0.2	6.91 ± 0.8
Upper Crust	10	2.80	2.20 ± 1.20	8.30 ± 4.90	2.70 ± 0.6	10.50 ± 1.0
Lower Crust	12	2.80	0.29 ± 0.24	3.17 ± 3.48	0.60 ± 0.4	3.70 ± 2.4

Table 3. Regional and Global suite of U and Th concentration distributed in the “Sediments”, Upper Crust and Lower Crust. *Data from Coltorti *et al.*⁵².

every 30 years)^{36,50,51}. The result is that up to 3.8×10^7 mol of He can be lost from mud volcanoes. Nonetheless these two outputs are less than about 10% of the amount of He stored in the main reservoir, does not entail any change in the conclusions, so it is reasonable to neglect their contribution in Eq. 1 which means an underestimation of the He present in the reservoir.

To compute ${}^4\text{He}_{\text{insitu}}$ and ${}^4\text{He}_{\text{External flux}}$ we used literature data for the abundances of U and Th and for crust thickness. Hence, we based our calculations on the U and Th amounts for a Regional Refined Reference Model and the Global Refined Reference Model (Table 3)⁵².

The *in-situ* production of ${}^4\text{He}$ is computed on the basis of the approach proposed by Zhou and Ballentine⁵³:

$${}^4\text{He}_{\text{insitu}} = \rho \times \Lambda \times \alpha \times (1 - \phi) \times V \times t \quad (2)$$

where ρ is the rock density in g/cm³ (2.21 g/cm³), Λ a parameter defining the efficiency of the transfer from the rock matrix into the gas phase, ϕ is the porosity of reservoir (fraction), α the source function of radioactive production of ${}^4\text{He}$ in the rock matrix (mol ${}^4\text{He}$ /grock/year), V the volume of the gas reservoir (cm³) and t the formation time of gas reservoirs (years). Since the process of ${}^4\text{He}$ released from a host mineral is short compared to the geologic age¹³ Λ can be regarded as being equal to 1. α , according to the U and Th decay equations, can be calculated using the following equation⁵⁴:

$$\alpha = 0.2355 \times 10^{-12} \times U \times [1 + 0.123 \times (Th/U - 4)] \quad (3)$$

where U and Th represent the concentrations of U and Th in rocks that host the reservoirs and are expressed in ppm. The accumulation rate of the *in situ* produced ${}^4\text{He}$ of gas reservoirs is expressed as (mol/y):

$$q_{\text{He}}^{\text{in}} = \rho \times \alpha \times (1 - \phi) \times V \quad (4)$$

The *in-situ* production of ${}^4\text{He}$ is 0.11 ± 0.02 mol/y and 0.30 ± 0.02 mol/yr (in Regional and Global model respectively).

The external flux of ${}^4\text{He}$ is computed by using the method in Zhou and Ballentine⁵³:

$${}^4\text{He}_{\text{External flux}} = q_{\text{He}}^{\text{c}}/S \times t \quad (5)$$

where S is the gas-bearing area of a reservoir (cm²), t the gas reservoir formation time (years) and q_{He}^{c} the average external crustal ${}^4\text{He}$ flux (mol ${}^4\text{He}$ /cm²/year). q_{He}^{c} can be calculated as:

$$q_{\text{He}}^{\text{c}} = \alpha \times \rho \times H \quad (6)$$

where ρ is the average crust density in g/cm³ (2.80 g/cm³)⁵⁵ and H is the crust thickness in cm (3.2×10^6 cm, Lavecchia *et al.* 2003)⁵⁶.

The external flux of ${}^4\text{He}$ to the two reservoirs is 37.53 ± 12.12 mol/y and 54.54 ± 5.86 mol/y (in Regional and Global model respectively, Fig. 4).

Considering these values of ${}^4\text{He}$ input in the reservoir, the total amount of ${}^4\text{He}$ that can be accumulated into the trap in a time going from 1.8 and 4.5 Myr, varies from 6.7×10^7 mol to 2.5×10^8 mol, respectively. These values are lower than the amount of He in the reservoir that we computed by using the volumetric method (from 3.64×10^8 mol to 4.12×10^8 mol, Table 3). So, production of ${}^4\text{He}$ from the whole crust below the main reservoir and its successive transfer by diffusion processes, cannot support the amount of He stored into the reservoirs (Fig. 5).

If we consider a steady-state diffusion model to explain the excess of ${}^4\text{He}$ in the two reservoirs we need to invoke a volume of ${}^4\text{He}$ -productive crust from 1.5 to 6.2 times larger than that below the trap (~ 1323 km³). Considering that previous investigations³⁸ highlighted that the source of CH₄ is in deep crustal layers (>3–6 km) and CH₄ vertically migrated towards the natural reservoirs it is reasonable that processes of volatiles migration different from the steady-state diffusion occurred below the investigated mud volcanoes systems.

${}^4\text{He}$ flux: Episodic degassing and active tectonic. The release of volatiles from rocks increases as effect of dilatancy and in regions affected by active tectonic, the flux of ${}^4\text{He}$ through the crust should be higher than that in un-deforming areas where it is reasonable to assume that a diffusive steady-state transport system is acting. Our calculations show that ${}^4\text{He}$ in the natural reservoirs is in excess respect to a steady-state whole crust degassing. As a result, in the main reservoir, there are between 1.2×10^8 and 3.5×10^8 moles in excess of the ${}^4\text{He}$ produced in the crust below the main reservoir plus the ${}^4\text{He}_{\text{insitu}}$.

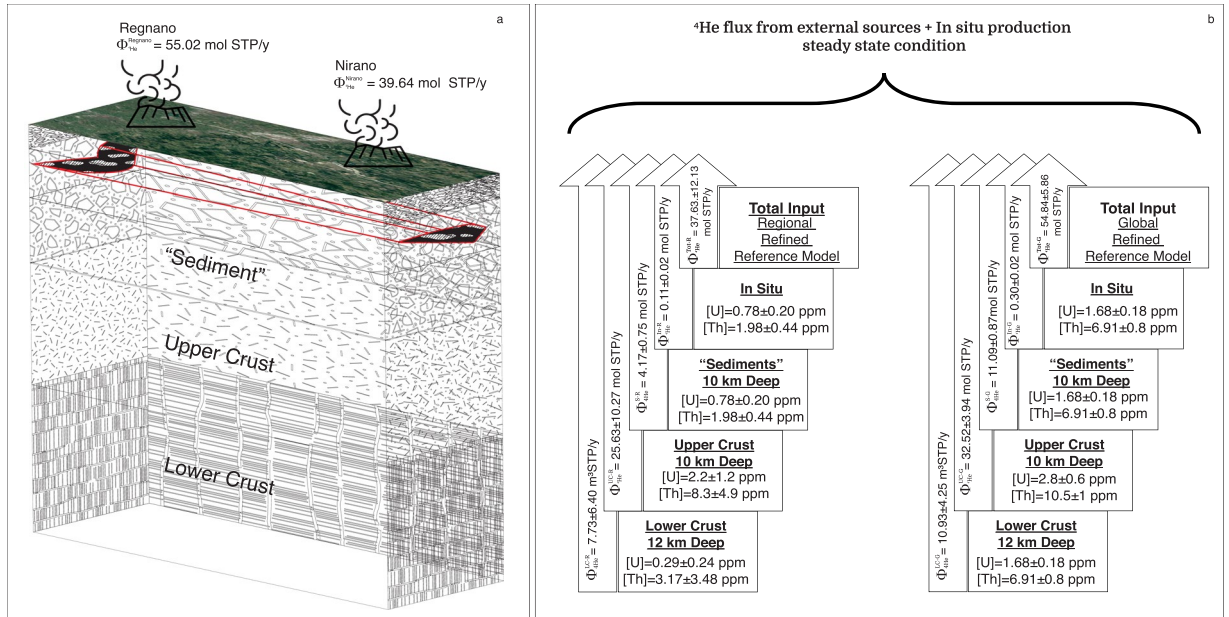


Figure 4. A simplified model of Nirano-Regnano mud volcanoes system. (a) Total input of crustal ^4He with concentrations of Uranium and Thorium ([U] and [Th], respectively) in “Sediment”, upper and lower crust. Data of [U] and [Th] contents in rocks from Coltorti *et al.*⁵². (b) Φ_{He}^{LC-G} and Φ_{He}^{LC-R} are the fluxes from the lower crust with [U] and [Th] content relative to the Regional (R) and Global (G) models. Φ_{He}^{UC-G} and Φ_{He}^{UC-R} are the fluxes from the upper crust with [U] and [Th] content relative to the Regional (R) and Global (G) models. Φ_{He}^{S-R} and Φ_{He}^{S-G} are the fluxes from the “Sediment” with [U] and [Th] content relative to the Regional (R) and Global (G) models. Φ_{He}^{In-G} and Φ_{He}^{In-R} are the fluxes from *in situ* production with [U] and [Th] content relative to the Regional (R) and Global (G) models. Φ_{He}^{Tot-G} and Φ_{He}^{Tot-R} are the total input flow that feeds the reservoir with [U] and [Th] content relative to the Regional (R) and Global (G) models. Φ_{He}^{Nirano} and $\Phi_{He}^{Regnano-R}$ are the total output flow from the mud volcanoes of Nirano and Regnano.

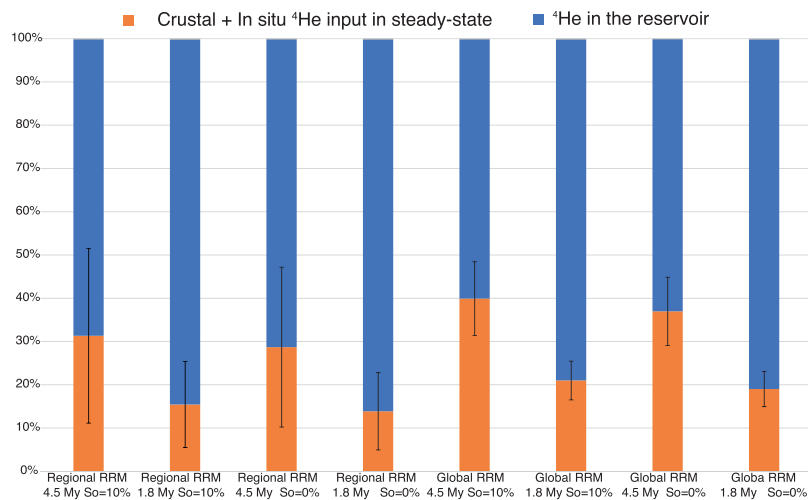


Figure 5. The production of radiogenic He and its release in stationary state, in the age of the trap (1.8 Ma or 4.5 Ma), represents from 15% to 40% of the helium present in the main reservoir. The error bars shown are 2σ .

Considering that the region is tectonically active and two main systems of active faults cross cut the deep reservoir (Fig. 2c and Methods: Geological setting), here we investigate if micro-fracturing can sustain the excess of ^4He in the reservoirs. The release of ^4He from rock, which are affected by dilatancy, is from 10 to 10^4 times higher than that in un-deformed rock²⁶, so the release of ^4He from a deforming fault damage zone is significantly higher if compared to the one of a tectonically undisturbed rock volume (Figs. 6 and S1).

The volume of the damage zones of the reservoir-related faults (from 0.015 km^3 to 0.088 km^3 ; Fig. 2) releases an amount of He that matches the excess of He in the reservoirs if the release of ^4He is 10^4 times higher than that produces by pure diffusion process occurring within an un-deformed rock volume (Figs. 6 and S1). However, the

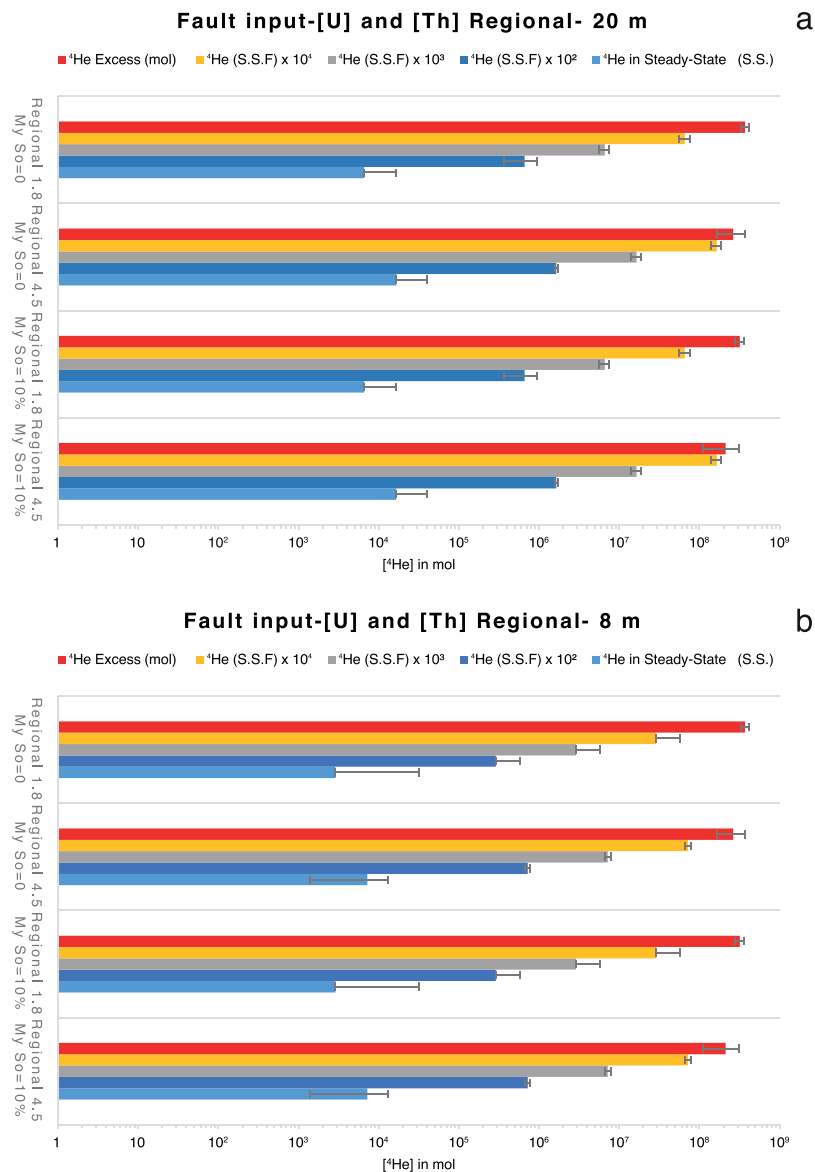


Figure 6. Fault contribution to the release of ^4He . Calculated ^4He released in Steady-state and S.S. $\times 10^3$ – 10^4 from faults system in Nirano (lateral extension 6250 m and length of the fault zone 300 m) and Regnano (lateral extension 8750 m and length of the fault zone 500 m) for a damage zone thickness of 20 m (a) and 8 m (b) with Regional U and Th contents.

high flux of volatiles from rocks as effect of dilatancy is not constant over time and it decreases in a scale of ka^{26} . It means that in order to produce a continuous flux of volatiles high enough to justify the amount of ^4He presumed to be into the reservoirs, the stress field has to be constantly active since the reservoir formation age. This result shows that the active regional tectonic could substantially contribute to enhance the ^4He flux within the reservoir and that it can be an additional process to sustain the amount of ^4He stored in the trap (Figs. 7 and S2). This implies that also the seismic activity is occurring since the origin of the gas traps.

Seismicity and degassing. We explored the hypothesis that the excess of He in the reservoirs may be due the occurrence of local earthquakes producing micro-fractures in crustal layers. Following the approach used by Sano *et al.*²⁸, which link the magnitude of an earthquake to the volume of rock affected by deformation and the related release of ^4He , we used the local (historical and instrumental) earthquakes activity as a proxy to calculate the amount of He released by the variation of the rock volume induced by each seismic event. We used the INGV database, covering the 1986–2018 time period (<http://cnt.rm.ingv.it>) for the instrumental earthquakes and the historical earthquakes catalogue (<https://emidius.mi.ingv.it>), covering the period 1501–1997, to compute the seismic energy released by the earthquakes located below the Nirano and Regnano systems. Moreover, we also extended the catalogue to the past (in terms of geological times), by assuming the same level of seismic energy release with time, from now up to the trap formation age. The considered events occurred at depths ranging

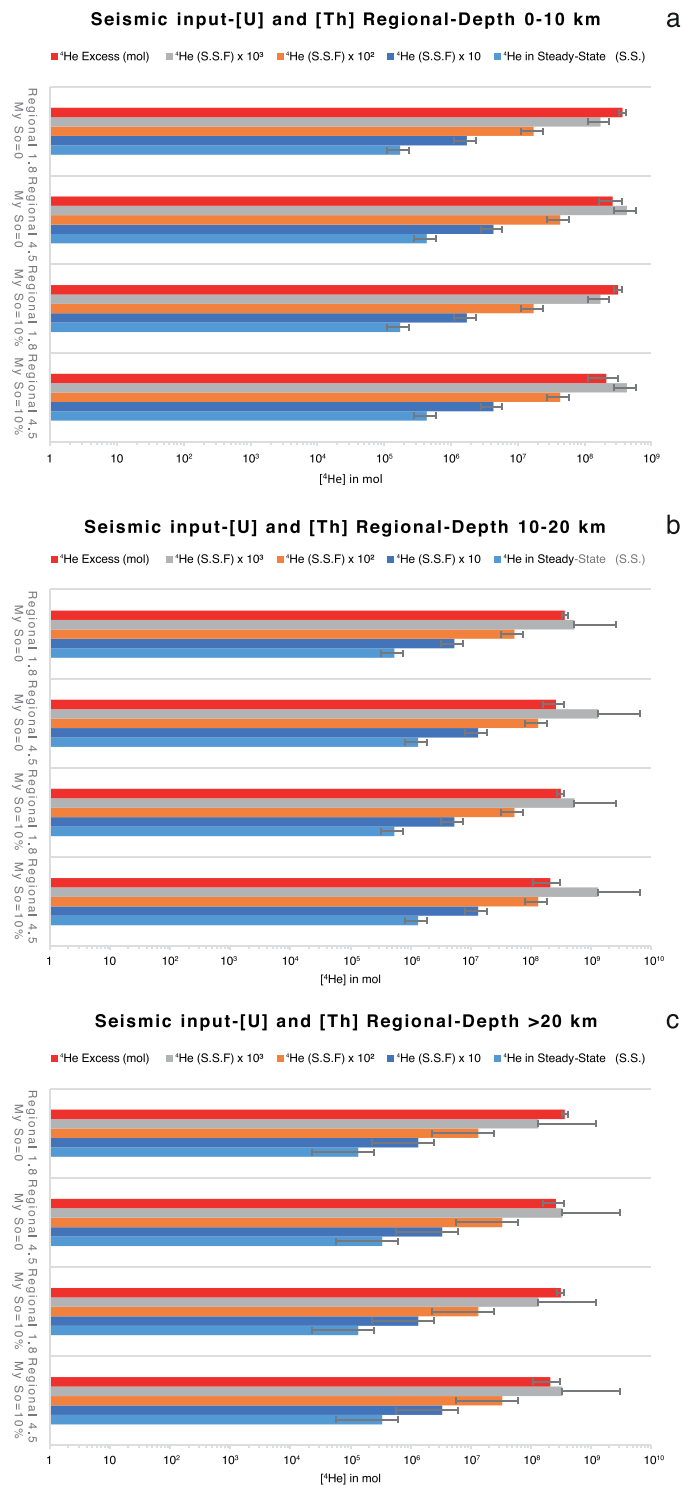


Figure 7. Seismic contribution to the release of ^4He . Calculated ^4He released in steady-state and S.S. $\times 10^3$ – 10^4 from deformed volume of rocks by earthquakes with average annual Mw calculated by means of estimated recurrence time after frequency-magnitude distribution by Zmap7 at 0–10 km depth (a) 10–20 km (b) and 20–32 km (c) for the uranium and thorium contents of the Regional suite.

between 5 km and 31 km and in 15 km wide sector along the axis of the anticline connecting Regnano to Nirano. We firstly converted the different types of magnitude reported in the catalogues (ML and Md) in moment magnitude (Mw). For the conversion from ML to Mw, we used the coefficients proposed by Castello *et al.*⁵⁷. While we converted the Md to Mw by using the coefficients proposed by Selvaggi *et al.*⁵⁸. We then computed the annual average of released energy (by using ZMAP computer code) for the analysis of seismic recurrences. The annual average of released energy is about 5.48×10^{16} ergs/y, which corresponds to one earthquake of magnitude equal

to 3.3 per year. Thus, we computed the average volume of rock deformed by the earthquakes per year^{28,59} by using the relationship:

$$\text{Log}V = 1.06M - 2.78 \quad (7)$$

where V and M are the volume of rock affected by seismicity (km^3) and the moment magnitude, respectively. These values correspond to a volume of deformed rock of 5.13 km^3 per year that is higher than the volume of the faults damage zones. The amount of He released from this volume are between 7.09×10^{-2} and $3.58 \times 10^{-2} \text{ mol/y}$ with a Regional or Global U and Th contents in the rock respectively. So, an increase of 3 orders of magnitude of the He released by the volume of deformed rocks, due to dilatancy^{26,43}, is still consistent to the amount of He estimated in the reservoirs (Figs. 7 and S2).

This result clearly indicates that the volume of deformed rock by stress field of the seismicity must be larger than the volume of the damage zone of the reservoir-related faults.

Conclusion

Our results show that the field of stress associated to the seismicity generated a release of ^4He from rock supporting the amount of ^4He that accumulated in the natural reservoirs since their formation (1.8–4.5 Ma). These results demonstrate that in tectonically active regions, the crustal ^4He degassing can episodically occur and powered as an advective process by seismo-genetic processes. In fact, in the studied area the ^4He flux through the crust towards the atmosphere is higher than that due to a steady-state diffusive degassing and this excess can be due to the local seismicity. Considering the recognized link between rock deformation/fracturation and He degassing, the monitoring of the He flux in seismically active regions can potentially provide evidences of a modification of the field of stress due to the active tectonics, so the He can provides information to a better knowledge of the seismo-genetic processes at regional scale. However, our study shows that natural reservoirs accumulate deep sourced volatiles and the natural traps work as a sponge over time by absorbing the signal transferred towards the surface by the volatiles coming from deeper than the reservoirs, so these volatiles do not quickly reach Earth surface. These results well fit with the evidences that the increase of the activity from the mud volcanoes or vents because of earthquake is essentially post-seismic, in the sense that it occurs as a consequence of earthquakes^{7,60} and generally, no geochemical variations are recognized before. Finally, mud volcanoes are surely preferential sites for studying the relationships between fluids and seismicity, however for using He and other volatiles to investigate the genesis of earthquakes it is fundamental to have a model of fluids circulation and its storage into the crust together with an high frequency monitoring of the He that outgases at the surface. The seismogenesis is a dynamic process of ongoing rock deformation until to the fracturation, so even if fluids are directly involved in these processes nevertheless the effects of rock deformation can be also masked or reach the surface in delay.

Methods

Analytical procedures. Gas samples were collected in Pyrex bottles with vacuum valves at both ends, taking care to prevent air contamination, and these were analysed in 10 days from their sampling. Gas samples have been analysed in the laboratories of the Istituto Nazionale di Geofisica e Vulcanologia, sezione di Palermo. The chemical composition of He, H_2 , O_2 , N_2 , CO, CH_4 , CO_2 and C_2H_6 has been measured by a Perkin Elmer Clarus 500 gas chromatograph equipped with a 3.5-m Carboxen 1000 column and double detector (hot-wire detector and flame ionization detector), with analytical errors of $<3\%$. Analytical precision for GC analyses is better than $\pm 5\%$ for trace gases and $\pm 10\%$ for alkanes. ^3He , ^4He and ^{20}Ne and the $^4\text{He}/^{20}\text{Ne}$ ratios were determined by separately admitting He and Ne into a split flight tube mass spectrometer (GVI-Helix SFT), after standard purification procedures⁶¹. $^3\text{He}/^4\text{He}$ ratio is expressed as R/Ra (being R the $^3\text{He}/^4\text{He}$ ratio of the sample, and Ra the $^3\text{He}/^4\text{He}$ ratio of air, 1.39×10^{-6}).

The analytical error is generally below 0.3%. The R/Ra values were corrected for the atmospheric contamination basing on the $^4\text{He}/^{20}\text{Ne}$ ratio⁶² and reported as Rc/Ra (Table 1)⁶³. The C isotope composition of CO_2 (expressed as $\delta^{13}\text{C}\text{‰}$ vs. V-PDB) was determined using a Thermo (Finnigan) Delta Plus XP CF-IRMS, connected to a Trace GC gas chromatograph and a Thermo (Finnigan) GC/C III interface^{63,64}. The gas chromatograph, equipped with a Poraplot-Q column (length 30 m, i.d. 0.32 mm), kept at a constant temperature of 50°C , uses He as the carrier gas. The analytical uncertainty was $\pm 0.1\text{‰}$. Carbon and hydrogen isotopes of CH_4 were carried out on the same equipment. GC III combustion interface was used to produce carbon dioxide from CH_4 ⁶⁵. GC-TC interface provides on-line high-temperature methane conversion into hydrogen suitable for isotope analyses. Typical reproducibility (1σ) for $\delta^{13}\text{C}-\text{CH}_4$ and $\delta\text{D}-\text{CH}_4$ measurements is better than 0.2‰ and 2.5‰ respectively⁶⁶.

Gas reserves computations. The classic approach to estimate the gas reserves stored in a natural reservoir (Q) is based on a volumetric method⁶⁷ where the computed values of the gases volume are statistically considered the “best-estimate” value⁶⁸. Here we applied this approach to compute the total amount of gas that is stored into the deep and shallow reservoirs (Table 2).

The total gas amount in the reservoir is computed by using the equation⁶⁹:

$$Q = \frac{G. B. V. \times \text{Net/Gross} \times \phi \times (1 - S_w - S_o)}{Bg} \quad (8)$$

where: G.B.V. = Gross Bulk Volume represents the gross volume of mineralized rock (inclusive of any clayey and/or compact horizons that do not contribute to production) ($9.5 \times 10^9 \text{ m}^3$ and $2.7 \times 10^8 \text{ m}^3$ the deep and the shallow gas reservoirs); Net/Gross = Ratio between the rock thickness that actually contributes to the production and

the gross thickness of rock (1 for this work); ϕ = Average porosity of the reservoir (fraction, 15%); S_w = Average water saturation of the “reservoir” (fraction) of Volume fraction of porosity filled with interstitial water⁷⁰; S_o = Oil saturation (between 0 and 10%); B_g = “Formation Volume Factor” that is used to express the volume of hydrocarbons originally in place at the “standard” surface conditions, i.e. at a pressure of 1 atm and at a temperature of 20 °C. The S_w it is equal to 15%, calculated with Timur 1968⁷¹. Where k is the permeability, equal to 80 mD.

$$S_w = \sqrt{\frac{10^4 \times \phi^{4.5}}{k}} \quad (9)$$

The Formation Volume Factor is given by the ratio of the volume of gas to the conditions of the reservoir and the volume of the gas to the standard conditions. Mathematically:

$$B_g = \frac{V_{rc}}{V_{sc}} = \frac{P_{sc} \times T_{rc} \times Z_{rc}}{P_{rc} \times T_{sc} \times Z_{sc}} \quad (10)$$

where, P_{sc} , T_{sc} , Z_{sc} , represent surface (pressure, temperature and compressibility factor) conditions while, P_{rc} , T_{rc} e Z_{rc} , are the conditions (pressure, temperature and compressibility factor) in the reservoir. The compressibility factor, Z , is calculated by using the approach in Piper and Corredor (1993)⁷². Therefore, the reverse of the Formation Volume Factor is equal to $1/B_g = 371.19$ SCM/ResCM, i.e. 1 m³ of pore volume under the reservoir conditions contains $1/B_g$ m³ of gas under standard conditions. Table 2 shows the total gas amount in the two reservoirs, Q: (1) from 1.66×10^{13} moles to 1.87×10^{13} moles for the deep reservoir (depth 1850–2600 m) at $P_{rc}^{Litho} = 49$ MPa, $T_{rc} = 327.15$ °K and S_o from 0 to 10% and (2) 2.36×10^{10} moles for the shallow trap (depth 400–1000 m) at $T_{rc} = 295.75$ °K, $P_{rc}^{Litho} = 4$ MPa $S_o = 0.0$. The lithostatic pressure were calculated taking into account the mean thicknesses and densities of the crustal layers and the value of g .

Helium lost by diffusion. The helium lost by diffusion it was calculated by one-dimensional steady-state diffusion model was used to quantify He loss in gas reservoirs using the formula in Liu *et al.*⁴⁹:

$$\int_0^t \frac{D}{Z} \left(\frac{22.4 \times Q \times C_{(t)}}{G. B. V. \times \phi \times K_{H_2O}} \times \frac{P_{NC} \times T_{RC}}{T_{NC}} - 4.5 \times 10^{-8} \right) \times S \times dt \quad (11)$$

where: D is the diffusion coefficient of He (2×10^{-6} cm²/s)⁴⁹; Z is the buried depth of reservoir, the middle point of deeper reservoir in this case (2225 m); Q is the total gas amount in the reservoir is computed by using the Eq. (8); $C_{(t)}$ is the ⁴He concentration at time t in %v; P_{NC} is the normal atmosphere (1 atm); T_{NC} is normal temperature (273 °K); T_{RC} is the reservoir condition temperature (327.15 °K); $G.B.V$ is the gross bulk volume in (9.49×10^{11} cm³); ϕ is the porosity (%); K_{H_2O} is the Henry’s constant calculated from the solubility model of noble gases in the water (approximately 2500)²⁴.

Received: 9 September 2019; Accepted: 21 November 2019;

Published online: 13 January 2020

References

- Torgersen, T. Continental degassing flux of ⁴He and its variability. *Geochem. Geophys. Geosystems* **11**, 1–15, <https://doi.org/10.1029/2009GC002930> (2010).
- Shen, B., Qin, J., Hu, W., Huang, Z. & Wang, J. Noble Gas Geochemistry of CO₂ Gas Pool in Gaoqing-Pingnan Fault Zone, Jiyang Depression. *Geol. J. China Univ.* **2009**, 537–546 (2009).
- Torgersen, T. & Clarke, W. B. Geochemical constraints on formation fluid ages, hydrothermal heat flux, and crustal mass transport mechanisms at Cajon Pass. *J. Geophys. Res.* **97**, 5031, <https://doi.org/10.1029/91JB01505> (1992).
- Etheridge, M. A., Wall, V. J., Cox, S. F. & Vernon, R. H. High fluid pressures during regional metamorphism and deformation: Implications for mass transport and deformation mechanisms. *J. Geophys. Res.* **89**, 4344–4358, <https://doi.org/10.1029/JB089iB06p04344> (1984).
- Tamburello, G., Pondrelli, S., Chiodini, G. & Rouwet, D. Global-scale control of extensional tectonics on CO₂ earth degassing. *Nat. Commun.* **9**, <https://doi.org/10.1038/s41467-018-07087-z> (2018).
- Chiodini, G. *et al.* Carbon dioxide Earth degassing and seismogenesis in central and southern Italy. *Geophys. Res. Lett.* **31**, n/a–n/a, <https://doi.org/10.1029/2004GL019480> (2004).
- Girault, F. *et al.* Persistent CO₂ emissions and hydrothermal unrest following the 2015 earthquake in Nepal. *Nat. Commun.* **9**, 1–10, <https://doi.org/10.1038/s41467-018-05138-z> (2018).
- Maestrelli, D. *et al.* Dynamic Triggering of Mud Volcano Eruptions During the 2016–2017 Central Italy Seismic Sequence. *J. Geophys. Res. Solid Earth* **122**, 9149–9165, <https://doi.org/10.1002/2017JB014777> (2017).
- Manga, M., Brumm, M. & Rudolph, M. L. Earthquake triggering of mud volcanoes. *Mar. Pet. Geol.* **26**, 1785–1798, <https://doi.org/10.1016/j.marpetgeo.2009.01.019> (2009).
- Holland, G. & Gilfillan, S. Application of Noble Gases to the Viability of CO₂ Storage. *Noble Gases as Geochem. Tracers*, 1–391, <https://doi.org/10.1007/978-3-642-28836-4> (2013).
- Parai, R. & Mukhopadhyay, S. Xenon isotopic constraints on the history of volatile recycling into the mantle, <https://doi.org/10.1038/s41586-018-0388-4> (2018).
- Avce, G., Marty, B. & Burgess, R. The origin and degassing history of the Earth’s atmosphere revealed by Archean xenon. *Nat. Commun.* **8**, 1–9, 1409.7398, <https://doi.org/10.1038/ncomms15455> (2017).
- Ballentine, C. J. & Burnard, P. G. Production, Release and Transport of Noble Gases in the Continental Crust. *Rev. Miner. Geochem.* **47**, 481–538, <https://doi.org/10.2138/rmg.2002.47.12> (2002).
- Ozima, M. & Podosek, F. *Noble Gas Geochemistry: 2nd edition* (Cambridge University Press, 2002).
- Mamyrin, B. A. & Tolstikhin, I. N. *Helium isotopes in nature*. Developments in Geochemistry (Elsevier Science Ltd, 1984).
- Allègre, C. J., Moreira, M. & Staudacher, T. ⁴He/³He dispersion and mantle convection. *Geophys. Res. Lett.* **22**, 2325–2328, <https://doi.org/10.1029/95GL02307> (1995).

17. Mabry, J., Lan, T., Burnard, P. & Bernard, M. High-precision helium isotope measurements in air. *J. Anal. At. Spectrom.* **28**, 1903–1910, <https://doi.org/10.1039/c3ja50155h> (2013).
18. Ballentine, C. J., Schoell, M., Coleman, D. & Cain, B. A. 300-Myr-old magmatic CO₂ in natural gas reservoirs of the west Texas Permian basin. *Nature* **409**, 327–331, <https://doi.org/10.1038/35053046> (2001).
19. O'Nions, R. K. & Oxburgh, E. R. Helium, volatile fluxes and the development of continental crust. *Earth Planet. Sci. Lett.* **90**, 331–347, [https://doi.org/10.1016/0012-821X\(88\)90134-3](https://doi.org/10.1016/0012-821X(88)90134-3) (1988).
20. Kulongoski, J. T. *et al.* Volatile fluxes through the Big Bend section of the San Andreas Fault, California: Helium and carbon-dioxide systematics. *Chem. Geol.* **339**, 92–102, <https://doi.org/10.1016/j.chemgeo.2012.09.007> (2013).
21. Caracausi, A. & Paternoster, M. Radiogenic helium degassing and rock fracturing: A case study of the southern Apennines active tectonic region. *J. Geophys. Res. Solid Earth*, 1–12, <https://doi.org/10.1002/2014JB011462> (2015).
22. Kennedy, B. M. *et al.* Mantle Fluids in the San Andreas Fault System, California. *Sci. (80-)* **278**, 1278 LP–1281, <https://doi.org/10.1126/science.278.5341.1278> (1997).
23. Kennedy, B. M. & van Soest, M. C. Flow of Mantle Fluids Through the Ductile Lower Crust: Helium Isotope Trends. *Sci. (80-)* **318**, 1433–1436, <https://doi.org/10.1126/science.1147537> (2007).
24. Ballentine, C. J., Burgess, R. & Bernard, M. Tracing Fluid Origin, Transport and Interaction in the Crust. *Rev. Miner. Geochem.* **47**, 539–614, <https://doi.org/10.2138/rmg.2002.47.13> (2002).
25. Bräuer, K., Geissler, W. H., Kämpf, H., Niedermann, S. & Rman, N. Helium and carbon isotope signatures of gas exhalations in the westernmost part of the Pannonian Basin (SE Austria/NE Slovenia): Evidence for active lithospheric mantle degassing. *Chem. Geol.* **422**, 60–70, <https://doi.org/10.1016/j.chemgeo.2015.12.016> (2016).
26. Torgersen, T. & O'Donnell, J. The degassing flux from the solid earth: Release by fracturing. *Geophys. Res. Lett.* **18**, 951–954, <https://doi.org/10.1029/91GL00915> (1991).
27. Sano, Y. *et al.* Groundwater helium anomaly reflects strain change during the 2016 Kumamoto earthquake in Southwest Japan. *Sci. Rep.* **6**, <https://doi.org/10.1038/srep37939> (2016).
28. Sano, Y., Takahata, N., Igarashi, G., Koizumi, N. & Sturchio, N. C. Helium degassing related to the Kobe earthquake. *Chem. Geol.* **150**, 171–179, [https://doi.org/10.1016/S0009-2541\(98\)00055-2](https://doi.org/10.1016/S0009-2541(98)00055-2) (1998).
29. Martinelli, G. & Judd, A. Mud volcanoes of Italy. *Geol. J.* **39**, 49–61, <https://doi.org/10.1002/gj.943> (2004).
30. Martinelli, G., Alberto, D. & Mucciarelli, M. Radon emissions from mud volcanoes in Northern Italy: possible connection with local seismicity. *Geophys. Res. Lett.* **22**, 1989–1992 (1995).
31. Rudolph, M. L. & Manga, M. Frequency dependence of mud volcano response to earthquakes. *Geophys. Res. Lett.* **39**, 1–5, <https://doi.org/10.1029/2012GL052383> (2012).
32. Martinelli, G. & Panahi, B. *Mud Volcanoes, Geodynamics and Seismicity*, vol. 51 (Springer, 2005).
33. Martinelli, G. & Dadomo, A. Mud Volcano Monitoring and Seismic Events. In Martinelli, G. & Panahi, B. (eds.) *Mud Volcanoes, Geodyn. Seism.*, 187–199 (Springer Netherlands, Dordrecht, 2005).
34. Etiope, G., Feyzulayev, A. & Baciu, C. L. Terrestrial methane seeps and mud volcanoes: A global perspective of gas origin. *Mar. Pet. Geol.* **26**, 333–344, <https://doi.org/10.1016/j.marpetgeo.2008.03.001> (2009).
35. Bonini, M. Interrelations of mud volcanism, fluid venting, and thrust-anticline folding: Examples from the external northern Apennines (Emilia-Romagna, Italy). *J. Geophys. Res. Solid Earth* **112**, 1–21, <https://doi.org/10.1029/2006JB004859> (2007).
36. Capozzi, R. & Picotti, V. Fluid migration and origin of a mud volcano in the Northern Apennines (Italy): The role of deeply rooted normal faults. *Terra Nov.* **14**, 363–370, <https://doi.org/10.1046/j.1365-3121.2002.00430.x> (2002).
37. Etiope, G., Martinelli, G., Caracausi, A. & Italiano, F. Methane seeps and mud volcanoes in Italy: Gas origin, fractionation and emission to the atmosphere. *Geophys. Res. Lett.* **34**, 1–5, <https://doi.org/10.1029/2007GL030341> (2007).
38. Sciarra, A., Cantucci, B., Ricci, T., Tomonaga, Y. & Mazzini, A. Geochemical characterization of the Nirano mud volcano, Italy. *Appl. Geochem.* **102**, 77–87, <https://doi.org/10.1016/j.apgeochem.2019.01.006> (2019).
39. Oppo, D., Capozzi, R. & Picotti, V. A new model of the petroleum system in the Northern Apennines, Italy. *Mar. Pet. Geol.* **48**, 57–76, <https://doi.org/10.1016/j.marpetgeo.2013.06.005> (2013).
40. Milkov, A. V. & Etiope, G. Revised genetic diagrams for natural gases based on a global dataset of >20,000 samples. *Org. Geochem.* **125**, 109–120, <https://doi.org/10.1016/j.orggeochem.2018.09.002> (2018).
41. Torgersen, T. & Clarke, W. B. Helium accumulation in groundwater, I: An evaluation of sources and the continental flux of crustal ⁴He in the Great Artesian Basin, Australia. *Geochim. Cosmochim. Acta* **49**, 1211–1218, [https://doi.org/10.1016/0016-7037\(85\)90011-0](https://doi.org/10.1016/0016-7037(85)90011-0) (1985).
42. Scholz, C. H., Sykes, L. R. & Aggarwal, Y. P. Earthquake Prediction: A Physical Basis. *Sci. (80-)* **181**, 803 LP–810, <https://doi.org/10.1126/science.181.4102.803> (1973).
43. Honda, M., Kurita, K., Hamano, Y. & Ozima, M. Experimental studies of He and Ar degassing during rock fracturing. *Earth Planet. Sci. Lett.* **59**, 429–436, [https://doi.org/10.1016/0012-821X\(82\)90144-3](https://doi.org/10.1016/0012-821X(82)90144-3) (1982).
44. Thomas, D. Geochemical precursors to seismic activity. *Pure Appl. Geophys. Pageoph* **126**, 241–266, <https://doi.org/10.1007/BF00878998> (1988).
45. Tapponier, P. & Brace, W. F. Development of stress induced microcracks in {W}esterly granite. *Int. J. Mech. Min. Sci. Geomech. Abstr.* **13**, 103–112, [https://doi.org/10.1016/0148-9062\(76\)91937-9](https://doi.org/10.1016/0148-9062(76)91937-9) (1976).
46. Bauer. Real Time Degassing of Rock during Deformation. No. SAND2016-1483C (2016).
47. Bauer, S. J., Gardner, W. P. & Heath, J. E. Helium release during shale deformation: Experimental validation. *Geochem. Geophys. Geosystems* **17**, 2612–2622, <https://doi.org/10.1002/2016GC006352> (2016).
48. Takahata, N. & Sano, Y. Helium flux from a sedimentary basin. *Appl. Radiat. Isot.* **52**, 985–992, [https://doi.org/10.1016/S0969-8043\(99\)00159-1](https://doi.org/10.1016/S0969-8043(99)00159-1) (2000).
49. Liu, W. *et al.* Formation time of gas reservoir constrained by the time-accumulation effect of ⁴He: Case study of the Puguang gas reservoir. *Chem. Geol.*, <https://doi.org/10.1016/j.chemgeo.2017.05.025> (2017).
50. Bonini, M. Mud volcano eruptions and earthquakes in the Northern Apennines and Sicily, Italy. *Tectonophysics* **474**, 723–735, <https://doi.org/10.1016/j.tecto.2009.05.018> (2009).
51. Martinelli, G. & Panahi, B. *Mud Volcanoes, Geodynamics and Seismicity: Proceedings of the NATO Advanced Research Workshop on Mud Volcanism, Geodynamics and Seismicity, Baku, Azerbaijan, from 20 to 22 May 2003*. Nato Science Series: IV: (Springer Netherlands, 2006).
52. Coltorti, M. *et al.* U and Th content in the Central Apennines continental crust: A contribution to the determination of the geoneutrinos flux at LNGS. *Geochim. Cosmochim. Acta* **75**, 2271–2294, 1102.1335, <https://doi.org/10.1016/j.gca.2011.01.024> (2011).
53. Zhou, Z. & Ballentine, C. J. ⁴He dating of groundwater associated with hydrocarbon reservoirs. *Chem. Geol.* **226**, 309–327, <https://doi.org/10.1016/j.chemgeo.2005.09.030> (2006).
54. Craig, H. & Lupton, J. E. Primordial neon, helium, and hydrogen in oceanic basalts. *Earth Planet. Sci. Lett.* **31**, 369–385, [https://doi.org/10.1016/0012-821X\(76\)90118-7](https://doi.org/10.1016/0012-821X(76)90118-7) (1976).
55. Rudnick, R. L. & Fountain, D. M. Nature and composition of the continental crust: A lower-crustal perspective. *Rev. Geophys.* **33**, 267–309, <https://doi.org/10.1029/95rg01302> (1995).
56. Lavecchia, G., Boncio, P., Creati, N. & Brozzetti, F. Some aspects of the Italian geology not fitting with a subduction scenario. *J. Virtual Explor.* **10**, 1–14, <https://doi.org/10.3809/jvirtex.2003.00064> (2003).

57. Castello, B., Olivieri, M. & Selvaggi, G. Local and duration magnitude determination for the Italian earthquake catalog, 1981–2002. *Bull. Seism. Soc. Am.* **97**, 128–139, <https://doi.org/10.1785/0120050258> (2007).
58. Selvaggi, G., Castello, B. & Azzara, R. Spatial distribution of scalar seismic moment release in Italy (1983–1996): seismotectonics implications for the Apennines (1997).
59. Shimazu, Y. *Physics of the Earth*. Shokabo Press (1971).
60. Manga, M. & Bonini, M. Large historical eruptions at subaerial mud volcanoes, Italy. *Nat. Hazards Earth Syst. Sci.* **12**, 3377–3386, <https://doi.org/10.5194/nhess-12-3377-2012> (2012).
61. Rizzo, A. L. *et al.* New mafic magma refilling a quiescent volcano: Evidence from He-Ne-Ar isotopes during the 2011–2012 unrest at Santorini, Greece. *Geochem. Geophys. Geosystems* **16**, 798–814, <https://doi.org/10.1002/2014GC005653> (2015).
62. Sano, Y. & Wakita, H. Geographical distribution of $^3\text{He}/^4\text{He}$ ratios in Japan: implications for arc tectonics and incipient magmatism. *J. Geophys. Res.* **90**, 8729–8741, <https://doi.org/10.1029/JB090iB10p08729> (1985).
63. Battaglia, A. *et al.* The Magmatic Gas Signature of Pacaya Volcano, With Implications for the Volcanic CO_2 Flux From Guatemala. *Geochem. Geophys. Geosystems* **19**, 667–692, <https://doi.org/10.1002/2017GC007238> (2018).
64. Gennaro, M. E., Grassa, F., Martelli, M., Renzulli, A. & Rizzo, A. L. Carbon isotope composition of CO_2 -rich inclusions in cumulate-forming mantle minerals from Stromboli volcano (Italy). *J. Volcanol. Geotherm. Res.* **346**, 95–103, <https://doi.org/10.1016/j.jvolgeores.2017.04.001> (2017).
65. Nuccio, P. M., Caracausi, A. & Costa, M. Mantle-derived fluids discharged at the Bradanic foredeep/Apulian foreland boundary: The Maschito geothermal gas emissions (southern Italy). *Mar. Pet. Geol.* **55**, 309–314, <https://doi.org/10.1016/j.marpetgeo.2014.02.009> (2014).
66. Carapezza, M. L. *et al.* Gas blowout from shallow boreholes near Fiumicino International Airport (Rome): Gas origin and hazard assessment. *Chem. Geol.* **407–408**, 54–65, <https://doi.org/10.1016/j.chemgeo.2015.04.022> (2015).
67. Tobergte, D. R. & Curtis, S. Assessment of Uncertainties in Oil and Gas Reserves Estimation by Various Evaluation Methods. *J. Chem. Inf. Model.* **53**, 1689–1699, arXiv:1011.1669v3, <https://doi.org/10.1017/CBO9781107415324.004> (2013).
68. Demirmen, F. Reserves Estimation: The Challenge for the Industry. *J. Pet. Technol.* **59**, 80–89, <https://doi.org/10.2118/103434-MS> (2007).
69. Mazzei, R. Calcolo volumetrico degli idrocarburi originariamente in posto. In *Elem. di Geol. e di Ing. dei giacimenti Pet.*, vol. FASCICOL07 (APEVE, 2001).
70. Mireault, R. & Dean, L. *Reservoir Engineering for Geologists*. (Fekete Associates Inc., 2012).
71. Timur, A. An Investigation of Permeability, Porosity, & Residual Water Saturation Relationships For Sandstone Reservoirs. *Log Anal.* **9**, 10 (1968).
72. Piper, L. D., McCain, W. D. & Corredor, J. H. Compressibility factors for naturally occurring petroleum gases. *SPE Repr. Ser.* 23–33, <https://doi.org/10.2118/26668-MS> (1999).
73. QGIS Development Team. QGIS Geographic Information System. Open Source Geospatial Foundation Project, <http://qgis.osgeo.org> (2019).
74. Gautheron, C. & Moreira, M. Helium signature of the subcontinental lithospheric mantle. *Earth Planet. Sci. Lett.* **199**, 39–47, [https://doi.org/10.1016/S0012-821X\(02\)00563-0](https://doi.org/10.1016/S0012-821X(02)00563-0) (2002).
75. Oppo, D. *Studio dei vulcani di fango per la definizione della migrazione dei fluidi profondi*. Ph.D. thesis, Università di Bologna Dipartimento (2011).

Acknowledgements

This work was supported by Istituto Nazionale di Geofisica e Vulcanologia, Grant FSE (Fondi Sociali Europei) and FISR (Fondo Integrativo Speciale per la Ricerca). A special thanks go to Dr. Giovanni Martinelli for providing us logistic support and collaboration into the collection of gases. We thank also INGV, Sezione di Palermo, for supplying the analytical support of all the analysis (gases chemistry, noble-gas and stable isotopes).

Author contributions

D.B., A.C. and R.F. designed the paper. A.C. collected the gases. D.B. developed all the calculations. D.B., A.C. and L.C. investigated the relationships between the earthquakes magnitude, rock fracturation and volatiles release. A.S. and M.G.M. provided all the geological information and the 3D reconstruction of the reservoirs. All the authors contributed in elaborating the data and writing the paper.

Competing interests

The authors declare no competing interests.

Additional information

Supplementary information is available for this paper at <https://doi.org/10.1038/s41598-019-55678-7>.

Correspondence and requests for materials should be addressed to D.B. or A.C.

Reprints and permissions information is available at www.nature.com/reprints.

Publisher's note Springer Nature remains neutral with regard to jurisdictional claims in published maps and institutional affiliations.



Open Access This article is licensed under a Creative Commons Attribution 4.0 International License, which permits use, sharing, adaptation, distribution and reproduction in any medium or format, as long as you give appropriate credit to the original author(s) and the source, provide a link to the Creative Commons license, and indicate if changes were made. The images or other third party material in this article are included in the article's Creative Commons license, unless indicated otherwise in a credit line to the material. If material is not included in the article's Creative Commons license and your intended use is not permitted by statutory regulation or exceeds the permitted use, you will need to obtain permission directly from the copyright holder. To view a copy of this license, visit <http://creativecommons.org/licenses/by/4.0/>.

© The Author(s) 2020